

## Adsorption of Cationic Lipid Bilayer onto Flat Silicon Wafers: Effect of Ion Nature and Concentration

Edla M. A. Pereira, Denise F. S. Petri, and Ana M. Carmona-Ribeiro\*

*Instituto de Química, Universidade de São Paulo, CP 26077, 05513-970 São Paulo SP, Brazil*

*Received: February 3, 2006; In Final Form: March 28, 2006*

The effect of monovalent salt nature and concentration over a range of low ionic strengths (0–10 mM LiCl, NaCl, KCl, or CsCl) and at two different pH values (6.3 and 10.0) on adsorption of dioctadecyldimethylammonium bromide (DODAB) bilayer fragments (BF) onto flat SiO<sub>2</sub> surfaces was systematically evaluated by means of in situ ellipsometry. High-affinity adsorption isotherms fitted by the Langmuir model indicated that adsorption maxima were consistent with bilayer deposition only around 10 mM monovalent salt at both pH values. In pure water, the mean thickness of the DODAB adsorbed layer was close to zero with bilayer deposition taking place only around 10 mM ionic strength. In the presence of 10 mM CsCl or LiCl, the highest and the lowest affinity constants for DODAB adsorption onto SiO<sub>2</sub> were, respectively, obtained consistently with the expected facility of cation exchange at the surface required for DODAB adsorption. The cation more tightly bound to the solid surface should be Li<sup>+</sup>, which would present the largest resistance to displacement by the DODAB cation, whereas the less tightly bound cation should be Cs<sup>+</sup> due to its largest ionic radius and lowest charge density. In other words, DODAB adsorption proceeds in accordance with charge density on the solid surface, which depends on the nature and concentration of bound counterions as well as DODAB cation ability to displace them. AFM images show a very smooth DODAB film adsorbed onto the surface in situ with a large frequency of BF auto-association from their edges. The present results for flat surfaces entirely agree with previous data from our group for DODAB adsorption onto silica particles.

### Introduction

Membrane-derivatized liquid–solid interfaces either on particles or on flat surfaces offer an extensive repertoire of chemical functionality.<sup>1–3</sup> However, the interaction between bilayer vesicles and mineral surfaces does not always produce the desired spreading, which is a single lipid bilayer on the support.<sup>4–8</sup> Cryo-TEM provided beautiful images of supported lipid bilayers on silica,<sup>9</sup> confirming previously obtained evidence from quantitative physicochemical methods such as determination of lipid adsorption isotherms,<sup>4–8</sup> dissipation of enhanced crystal-quartz microbalance (QCM-D),<sup>3,10–12</sup> surface plasmon resonance,<sup>1</sup> ellipsometry,<sup>13</sup> or atomic force microscopy.<sup>14,15</sup> The cationic lipid DODAB is special due to its anti-microbial properties and the additional possibility of direct immobilization of oppositely charged biomolecules or other biological structures.<sup>2</sup> These special properties justify this systematic study of DODAB bilayer fragment adsorption on silicon wafers. Furthermore, one should recall that DODAB bilayer fragments (BF) have recently found many applications in drug delivery or as interface agents that cover particles with cationic bilayers.<sup>16</sup>

In this work, by means of in situ ellipsometry, at pH 6.3 or 10.0, the effect of monovalent salt nature and concentration (0–10 mM LiCl, NaCl, KCl, or CsCl) on the adsorption of dioctadecyldimethylammonium bromide (DODAB) from bilayer fragments onto flat SiO<sub>2</sub> surfaces is systematically evaluated. DODAB adsorption proceeds in accordance to charge density of the solid surface, which depends on the nature and concentration of bound counterions as well as the DODAB cation ability to displace them. The results entirely agree with previous data

from our group for DODAB adsorption on silica<sup>4–6</sup> and with previous data on the adsorption of quaternary ammonium cations on mica from Pashley and co-workers.<sup>17,18</sup> AFM images of adsorbed DODAB BF in situ evidenced auto-associated bilayer fragments forming a very smooth film on the surface.

### Experimental Procedures

Dioctadecyldimethylammonium bromide (DODAB), 99.9% pure, was purchased from Sigma and used as received. Small DODAB bilayer fragments were prepared by ultrasonically dispersing the DODAB powder with a macrotip probe in Milli-Q water, pH 6.5, at 2.0 mM DODAB (nominal potency 80 W/15 min of sonication time) as previously described.<sup>19</sup> Following sonication, the solutions were centrifuged (10 000g/15 °C/40 min) to eliminate the titanium ejected from the tip. Mean zeta-averaged diameter and zeta-potential for the DODAB dispersions in pure water were 80 ± 1 nm and 43 ± 1 mV, respectively. The DODAB concentration was determined from bromide microtitration.<sup>20</sup> Monovalent salts, LiCl, NaCl, NaOH, KCl, and CsCl, 99.9% pure, were purchased from Merck (Darmstadt, Germany) or Sigma. All other chemicals were analytical grade and used without further purification. For adjusting the pH value to 10, 10 mM NaOH was used under a nitrogen atmosphere. Water was Milli-Q quality.

Silicon (100) wafers were purchased from Crystec (Berlin, Germany) with a native oxide layer approximately 2 nm thick and were rinsed in accordance with previously described protocols.<sup>21,22</sup>

As a control, first the thickness of the clean silicon wafers was measured in air (ex situ) and then in situ by immersion in

\* To whom correspondence should be addressed. Tel.: 55 11 3091 3810, ext 237. Fax: 55 11 3815 5579. E-mail: mcribeir@iq.usp.br.

25 mL of pure water or 20 mM monovalent salt solution either at pH 6.3 or 10. Thereafter, a volume of 12.5 mL of water and/or salt solutions was withdrawn from the trapezoidal ellipsometric cell, and 12.5 mL of DODAB BF aqueous dispersion was added, so that the final concentration of monovalent salt amounted to 10 mM.

Ellipsometric measurements were performed *ex situ* (in air) or *in situ* (in water or salt solution) using a vertical computer-controlled DRE-EL02 Ellipsometer (Ratzeburg, Germany). The angle of incidence was set to 70.0°, and the wavelength of the laser was 632.8 nm with an incidence area of 3 mm<sup>2</sup>. Adsorption from the solution was monitored *in situ* with a trapezoidal poly-(tetrafluoroethylene) cell described elsewhere.<sup>23</sup> At a controlled temperature (22–23 °C), ellipsometric angles  $\Delta$  and  $\Psi$  were measured and recorded at intervals of 4 s. The adsorption time required to obtain constant values for  $\Delta$  and  $\Psi$  was approximately 15 min. For the interpretation of the ellipsometric angles  $\Delta$  and  $\Psi$ , a multilayer model was used, assuming a refractive index  $n$  for Si as a complex number equal to 3.858–0.018i, where 0.018i is the imaginary component of the refractive index: for SiO<sub>2</sub>, 1.462; for the DODAB layer, 1.500; and for the bulk solution, 1.333, as measured by an Abbé refractometer. If the adsorbed lipid layer is regarded as a homogeneous film, the thickness can be calculated by iterative calculations with Jones' matrices.<sup>24–28</sup> As reviewed previously,<sup>25</sup> despite the low optical contrast for adsorbed surfactant layers relative to the aqueous bulk solution, ellipsometry has been successfully applied for *in situ* determinations of properties of thin adsorbed surfactant films<sup>27,28</sup> other than the adsorbed amount by accurately determining the optical properties of the multilayer substrate, like the surfactant/SiO<sub>2</sub>/Si layers, in different ambient media (air and water).

From the ellipsometric angles  $\Delta$  and  $\Psi$  (constant values after 15 min of adsorption), a multilayer model composed of Si, SiO<sub>2</sub>, the DODAB layer, the bulk solution, and the iterative calculations,<sup>24,26,27</sup> it is possible to determine the average thickness of the uppermost DODAB layer,  $d$ , both statically and dynamically. One should notice that each layer is usually characterized sequentially regarding independent ellipsometric determinations of thickness and refractive index.<sup>27,28</sup> One should also notice that ellipsometry enables the independent determination of  $n$  and  $d$ , only if the optical contrast in the system is large enough or if the layer thickness is thick enough. When  $\lambda$  is 633 nm and  $d \gg 30$  nm, it is possible to obtain  $n$  and  $d$  for the uppermost layer independently. However, in the present system,  $d \ll 30$  nm for the uppermost lipid layer, so that  $n$  must be assumed as  $n = 1.500$ , the usual value for a hydrocarbon layer, and  $d$  is calculated from ellipsometric angles and the multilayer model plus independent determinations of thicknesses and refractive indices for each layer.

The surface coverage  $\Theta$  was calculated by dividing the thickness  $d$  measured at a given DODAB concentration and the thickness at a limiting adsorption  $d_{\max}$

$$\Theta = \frac{d}{d_{\max}} \quad (1)$$

The dependence of  $\Theta$  on DODAB concentration could be described by the Langmuir adsorption model

$$\Theta = \frac{KC_{\text{DODAB}}}{(1 + KC_{\text{DODAB}})} \quad (2)$$

where  $C_{\text{DODAB}}$  is the concentration of DODAB in solution and

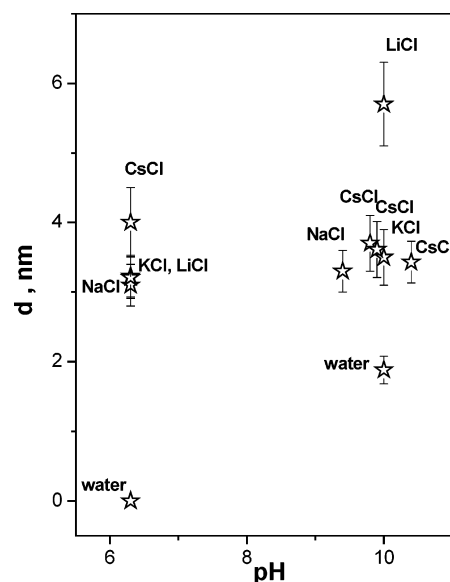


**Figure 1.** Mean adsorbed DODAB layer thickness ( $d$ ) on SiO<sub>2</sub> wafers from 0.4 mM DODAB BF dispersion in water or 10 mM monovalent salt, around two pH values (6.3 and 10.0).

$K$  is the affinity constant. The larger  $K$  is, the higher the affinity between substrate and adsorbate is.

AFM topographic images were obtained using a PicoSPM-LE Molecular Imaging system with cantilevers operating in the intermittent-contact mode (AAC mode), slightly below their resonance frequency of approximately 90 kHz in the fluid cell or 290 kHz in air. All topographic images represent unfiltered original data. At least two samples of the same material were analyzed at different areas of the surface. Surface roughness was evaluated from roughness mean square (rms) determinations over a specified surface area.

## Results and Discussion

Figure 1 shows mean layer thicknesses of adsorbed DODAB onto flat SiO<sub>2</sub> wafers at pH 6.3 and around 10.0 in pure water or 10 mM monovalent salts. In pure water at pH 6.3, there is no DODAB adsorption onto the wafers, possibly because the surface potential on the surface was not high enough as to drive DODAB deposition onto the surface in exchange for hydronium ions. This agrees with adsorption isotherms previously obtained for DODAB adsorption on silica particles in pure water at pH 6.3, which also indicated a similar absence of DODAB adsorption (or adsorption at very low levels).<sup>4–6</sup> In contrast, upon increasing the pH to 10.0, the DODAB layer mean thickness reaches 1.9 nm, in accordance with the expected increase in surface charge due to the increased silanol dissociation (Figure 1). Interestingly enough, DODAB adsorption amounted to mean thicknesses compatible with bilayer adsorption, ca. 4.0 nm, just when the ionic strength was increased to 10 mM monovalent salt for all salts tested both at pH 6.3 and 10 (Figure 1). This result can be understood from an increase in surface charge density upon increasing the ionic strength from zero to 10 mM monovalent salt. In the special case of LiCl, where Li<sup>+</sup> is the more hydrated and easily exchangeable cation, the largest DODAB adsorption occurs (Figure 1). These results closely resemble those obtained by Pashley in the early eighties for surface charging/ion exchange properties of mica, which were accurately described by a simple mass-action (site-binding) model.<sup>17</sup> Later on, Claesson and co-workers<sup>29</sup> compared adsorption densities on the isolated mica surface with those observed on forcing two opposing mica sheets together and concluded

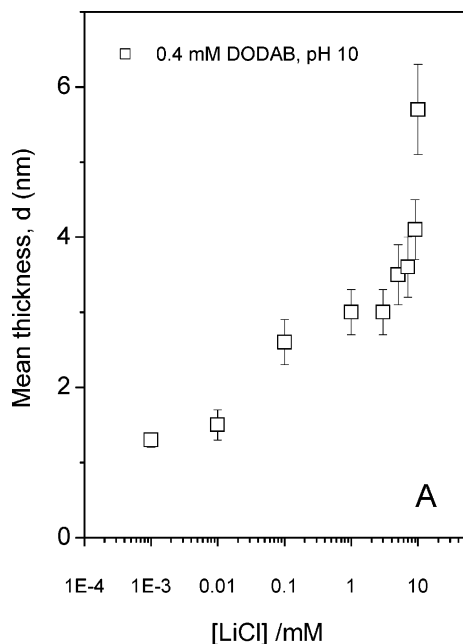


**Figure 2.** Effect of LiCl concentration on mean DODAB layer thickness ( $d$ ) adsorbed on SiO<sub>2</sub> wafers from 0.4 mM DODAB BF dispersion in water solution at pH 10.0.

that their data supported the hypothesis that in diluted solutions, hydrated ions can be exchanged and replaced by less hydrated ions under pressure, whereas in more concentrated solutions, this displacement would be prevented. The present results are consistent with the displacement of all tested cations by the less hydrated DODAB cation.

The effect of LiCl concentration (0–10 mM) at pH 10 on mean layer thickness of adsorbed DODAB from 0.4 mM DODAB bilayer fragments onto the SiO<sub>2</sub> flat surface is shown Figure 2. The DODAB adsorption increases with ionic strength over the range of 0.001–10.0 mM, displaying a linear dependence ( $R = 0.94$ ) with the square root of LiCl concentration (not shown). Therefore, DODAB adsorption is driven by the increase in surface charge density on the surface that takes place upon increasing ionic strength. In Figure 1, the dominance of the ionic strength over pH effect was demonstrated over a range of low ionic strengths. Increasing the ionic strength increases silanol dissociation, surface charge density, and DODAB adsorption.

In the diffuse layer, the Gouy–Chapman model assumes that ions interact with the surface only via the electrostatic mean field potential originating from the ion distribution itself and a smeared out surface charge.<sup>30</sup> Stern<sup>31</sup> improved the model by including also counterion adsorption to the surface so that the double-layer force originates from a plane one ion diameter further out. To investigate the effect of different monovalent cations on DODAB adsorption at the solid surface, adsorption isotherms for DODAB from DODAB BF onto the SiO<sub>2</sub> surface were obtained at pH 10 and 10 mM CsCl (Figure 3) or LiCl (Figure 4). There is a high-affinity constant with a limiting adsorption layer of 4.0–5.7 nm that is compatible with bilayer deposition in both cases (Figures 3 and 4 and Table 1). However, the affinity constant  $K$  for DODAB adsorption in the presence of 10 mM CsCl is higher than the one obtained in the presence of 10 mM LiCl. The cation that is more easily displaced by the DODAB cation is Cs<sup>+</sup>, which is the one with the lowest charge/cation radius ratio (Figure 5). One should notice that the charge/ion radii in Figure 5 are those obtained in the solid and crystalline monovalent salts by X-ray diffraction methods<sup>32</sup> and

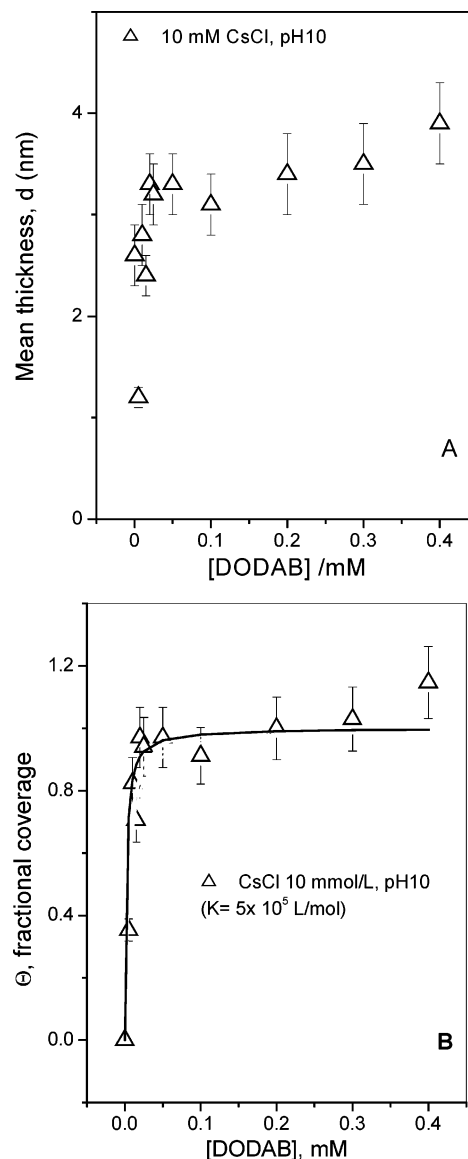


**Figure 3.** Isotherm for DODAB adsorption from DODAB BF on SiO<sub>2</sub> wafers at 10 mM CsCl and pH 10. Adsorption was expressed either as mean adsorbed thickness (A) or fractional coverage ( $\Theta$ ) with the continuous line calculated from Langmuir model by assuming  $K$  as  $5 \times 10^5$  L/mol (B).

that the ionic radii do not include the usual hydration layer surrounding the cations in aqueous solution. Despite the lower affinity constant for DODAB adsorption on the surface in the presence of 10 mM LiCl than the one obtained in the presence of 10 mM CsCl, the contrary was observed for the limiting adsorption, which was higher in LiCl (Table 1). Thicknesses for the adsorbed DODAB bilayer are 5.7 in 10 mM LiCl and 3.7–4.0 nm in 10 mM other monovalent salts (Figures 1, 3, and 4). Possibly, the larger DODAB thickness in the presence of LiCl was due to adsorption taking place without complete removal of the hydrated lithium layer between the DODAB bilayer and the solid surface.

The stability of dioctadecyldimethylammonium bromide Langmuir–Blodgett films on mica in aqueous salt solutions was studied by surface force measurements and atomic force microscopy (AFM).<sup>33</sup> There was a surface charge dependency on salt concentration as well as breakdown and hydrophilization of the Langmuir–Blodgett film when surfaces were brought into contact in high salt concentrations. AFM images of untreated films showed small holes and breakdown when

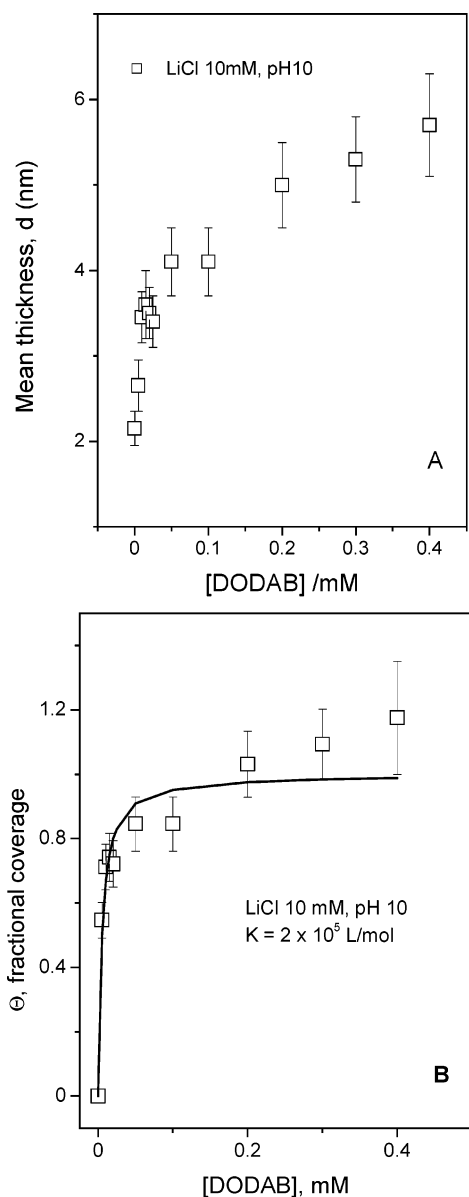


**Figure 4.** Isotherm for DODAB adsorption from DODAB BF on SiO<sub>2</sub> wafers at 10 mM LiCl and pH 10. Adsorption was expressed either as mean adsorbed thickness (A) or fractional coverage  $\Theta$  with the continuous line calculated from Langmuir model by assuming  $K$  as  $2 \times 10^5$  L/mol (B).

**TABLE 1: Adsorption Parameters for DODAB Adsorption from Bilayer Fragments onto SiO<sub>2</sub> Flat Substrates at pH 10 and 10 mM Monovalent Salt**

| monovalent salt | affinity constant, $K$ (L/mol) | mean thickness at maximal adsorption, $d_{\max}$ (nm) |
|-----------------|--------------------------------|---|
| LiCl            | $2 \times 10^5$                | $5.7 \pm 0.6$   |
| CsCl            | $5 \times 10^5$                | $3.9 \pm 0.4$   |

exposed to salt solutions.<sup>33</sup> The present results show that possibly the DODAB bilayer fragments adsorb onto the wafer via multipoint attachment in a manner resembling polyelectrolyte adsorption onto surfaces at low ionic strengths. In fact, it was previously shown that for a strongly charged polyelectrolyte in a low salt solution, the adsorbed amount scales as the square root of the ionic strength,<sup>34</sup> similarly to DODAB BF adsorption onto the wafer (Figure 2).

The Supporting Information shows AFM topographic images obtained in the air for a bare silicon wafer, DODAB BF

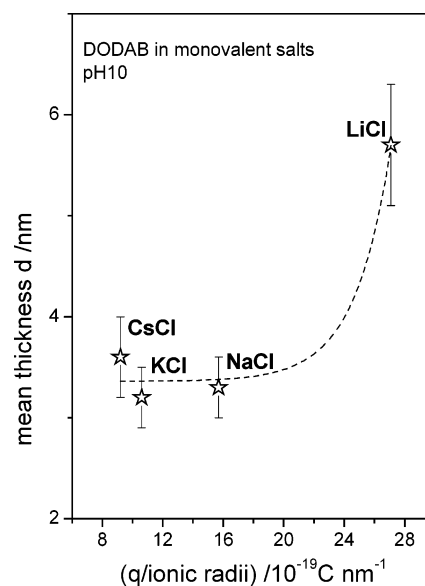


**Figure 5.** Mean adsorbed DODAB layer thickness ( $d$ ) on SiO<sub>2</sub> wafers from 0.4 mM DODAB BF dispersion in 10 mM monovalent salt, at pH 10.0, as a function of the ratio between cation charge and radius. The ionic radii were taken from crystallographic determinations.<sup>32</sup>

adsorbed onto Si wafers from a 0.4 mM DODAB BF dispersion in LiCl 10 mM and pH 10, and in situ images of DODAB BF adsorbed onto Si wafers from a 0.4 mM DODAB BF dispersion in LiCl 10 mM and pH 10. The DODAB BF are scarcely seen as separate entities, instead evident worm-like structures (the brightest spots) are observed as the result of BF edges self-assembling. One should recall that the deepest points (the darkest spots) do not necessarily represent that the tip touched the bare wafer, so that the  $z$  scale does not represent the absolute film thickness. For the covered surface, the deepest level is not available from the topography, which mainly evaluates roughness. Roughness mean square (rms) for bare SiO<sub>2</sub> surface under air, DODAB-covered SiO<sub>2</sub> dried and under air, and DODAB BF-covered SiO<sub>2</sub> in water are 0.17 nm, 0.36 nm ( $5 \mu\text{m} \times 5 \mu\text{m}$ ), and 0.20 nm ( $1 \mu\text{m} \times 1 \mu\text{m}$ ), respectively. Under air, topography was not smooth. On the other hand, in situ, a very smooth surface occurred. Self-assembled DODAB structures can be easily identified in situ. The surface is typically very smooth and flat, increasing the level of noise. Similar noisy images can be obtained for bare Si wafer, a surface smoother than those presented in this paper. One should notice that images were not filtered to eliminate the noise and that the noise is a consequence of the very smooth surface obtained for a DODAB BF-covered wafer. The topography of adsorbed DODAB BF in 10 mM LiCl, pH 10, in situ (without draining or drying after adsorption), shows regions of ordered worm-like structures approximately 70 nm broad, consistent with the 80 nm mean diameter of DODAB BF.

Sligar and co-workers have described interesting bilayer fragments stabilized by membrane scaffold proteins, which surrounded a lipid bilayer in a belt-like fashion, forming bilayer disks of discrete size and composition.<sup>35,36</sup> They obtained AFM images for these structures that were distinct from the images shown for DODAB BF in the Supporting Information. In their case, the fragments remained perfectly isolated and did not seem to have auto-associated on the solid surface since hydrophilic domains of the belt-like protein would have prevented such auto-association.



## Conclusion

High-affinity adsorption isotherms for the cationic lipid DODAB onto silicon wafers were fitted by the Langmuir model with adsorption maxima consistent with bilayer deposition only around 10 mM monovalent salt at pH 6.3 or 10.0. In pure water, the mean thickness of the DODAB adsorbed layer was close to zero, with bilayer deposition taking place only around 10 mM ionic strength. In the presence of 10 mM CsCl or LiCl, the highest and lowest affinity constants for DODAB adsorption onto SiO<sub>2</sub> were, respectively, obtained consistently with the expected facility of cation exchange at the surface required for DODAB adsorption. The cation more tightly bound to the solid surface should be Li<sup>+</sup>, which would present the largest resistance to displacement by the DODAB cation, whereas the less tightly bound should be Cs<sup>+</sup> due to its largest ionic radius and lowest charge density. In other words, DODAB adsorption proceeds in accordance with charge density on the solid surface, which depends on the nature and concentration of bound counterions as well as DODAB cation ability to displace them. The Hofmeister series is a list of ions rank-ordered in terms of how strongly they modulate the hydrophobicity of a nonpolar solute (hydrophobe) in a water solution.<sup>37–40</sup> Small ions tend to cause salting out, that is, they reduce hydrophobic solubilities in water, whereas large ions tend to cause salting-in, increasing nonpolar solubilities. The Hofmeister series, however, does not correlate perfectly with ionic charge density: while lithium is smaller than sodium, lithium has a weaker Hofmeister effect.<sup>37–40</sup> In the present case, DODAB more easily displaced cesium than the lithium ion, meaning that Li<sup>+</sup> was more strongly bound to the silicon wafer than Cs<sup>+</sup> in clear agreement with expected results from the Hofmeister series. Certainly, in this case, counterion hydration is less important in determining the exchange between DODA cation and bound cation than the net ionic charge density. AFM images show a very smooth DODAB film adsorbed onto the surface in situ with a large frequency of BF auto-association from their edges. The ionic strength is a key factor in determining DODAB BF adsorption on the silicon wafer, a conclusion similar to the one previously achieved for DODAB adsorption on silica particles.

**Acknowledgment.** FAPESP and CNPq are gratefully acknowledged for financial support. The authors thank Priscila M. Kosaka for her help during the AFM measurements.

**Supporting Information Available:** AFM topographic images of bare silicon wafer in air and DODAB BF adsorbed onto the wafer after drying or DODAB BF adsorbed onto the wafer in situ (in aqueous solution). This material is available free of charge via the Internet at <http://pubs.acs.org>.

## References and Notes

- (1) Knoll, W. *Annu. Rev. Phys. Chem.* **1998**, *49*, 569.
- (2) Carmona-Ribeiro, A. M. *Chem. Soc. Rev.* **2001**, *30*, 241–247.
- (3) Richter, R.; Mukhopadhyay, A.; Brisson, A. *Biophys. J.* **2003**, *85*, 3035–3047.
- (4) Rapuano, R.; Carmona-Ribeiro, A. M. *J. Colloid Interface Sci.* **1997**, *193*, 104–111.
- (5) Rapuano, R.; Carmona-Ribeiro, A. M. *J. Colloid Interface Sci.* **2000**, *226*, 299–307.
- (6) Moura, S. P.; Carmona-Ribeiro, A. M. *Langmuir* **2003**, *19*, 6664–6667.
- (7) Moura, S. P.; Carmona-Ribeiro, A. M. *Langmuir* **2005**, *21*, 10160–10164.
- (8) Moura, S. P.; Carmona-Ribeiro, A. M. *Cell Biochem. Biophys.* **2006**, *44*, 446–452.
- (9) Mornet, S.; Lambert, O.; Duguet, E.; Brisson, A. *Nano Lett.* **2005**, *5*, 281–285.
- (10) Reimhult, E.; Hoeoek, F.; Kasemo, B. *Langmuir* **2003**, *19*, 1681–1691.
- (11) Seantier, B.; Breffa, C.; Felix, O.; Decher, G. *J. Phys. Chem. B* **2005**, *109*, 21755–21765.
- (12) Boudard, S.; Seantier, B.; Breffa, C.; Decher, G.; Felix, O. *Thin Solid Films* **2005**, *495*, 246–251.
- (13) Benes, M.; Billy, D.; Hermens, W. T.; Hof, M. *Biol. Chem.* **2002**, *383*, 337–341.
- (14) Reviakine, I.; Brisson, A. *Langmuir* **2000**, *16*, 1806–1815.
- (15) Jass, J.; Tjaernhage, T.; Puu, G. *Biophys. J.* **2000**, *79*, 3153–3163.
- (16) Carmona-Ribeiro, A. M. *Curr. Med. Chem.* **2006**, *13*, 1359–1370.
- (17) Pashley, R. M. *J. Colloid Interface Sci.* **1981**, *80*, 531–545.
- (18) Claesson, P.; Horn, R. G.; Pashley, R. M. *J. Colloid Interface Sci.* **1984**, *100*, 250–263.
- (19) Carmona-Ribeiro, A. M. *Chem. Soc. Rev.* **1992**, *21*, 209–214.
- (20) Schales, O.; Schales, S. S. *J. Biol. Chem.* **1941**, *140*, 879–884.
- (21) Motschmann, H.; Stamm, M.; Toprakcioglu, C. *Macromolecules* **1991**, *24*, 3681–3688.
- (22) Siqueira, D. F.; Reiter, J.; Breiner, U.; Stadler, R.; Stamm, M. *Langmuir* **1996**, *12*, 972–979.
- (23) Fujimoto, J.; Petri, D. F. S. *Langmuir* **2001**, *17*, 56–60.
- (24) Azzam, R. M. A.; Bashara, N. M. *Ellipsometry and Polarized Light*; North-Holland: Amsterdam, 1987.
- (25) Tiberg, F.; Landgren, M. *Langmuir* **1993**, *9*, 927–932.
- (26) Pereira, E. M. A.; Petri, D. F. S.; Carmona-Ribeiro, A. M. *J. Phys. Chem. B* **2002**, *106*, 8762–8767.
- (27) Tiberg, F.; Jonsson, B.; Lindman, B. *Langmuir* **1994**, *10*, 3714–3722.
- (28) Tiberg, F.; Jonsson, B.; Tang, J.; Lindman, B. *Langmuir* **1994**, *10*, 2294–2300.
- (29) Claesson, P. M.; Herder, P.; Stenius, P.; Eriksson, J. C.; Pashley, R. M. *J. Colloid Interface Sci.* **1986**, *109*, 31–39.
- (30) Israelachvili, J. N. *Intermolecular and Surface Forces*, 2nd ed.; Academic Press Inc.: San Diego, 1992.
- (31) Stern, O. Z. *Electrochemistry* **1924**, *30*, 508.
- (32) Shannon, R. D. *Acta Crystallogr.* **1974**, *A32*, 751.
- (33) Eriksson, L. G. T.; Claesson, P. M.; Ohnishi, S.; Hato, M. *Thin Solid Films* **1997**, *300*, 240–255.
- (34) Borukhov, I.; Andelman, D.; Orland, H. *Macromolecules* **1998**, *31*, 1665–1671.
- (35) Shaw, A. W.; McLean, M. A.; Sligar, S. G. *FEBS Lett.* **2004**, *556*, 260.
- (36) Bayburt, T. H.; Grinkova, Y. V.; Sligar, S. G. *Nano Lett.* **2002**, *2*, 853.
- (37) Collins, K. D. *Proc. Natl. Acad. Sci.* **1995**, *92*, 5553–5557.
- (38) Hribar, B.; Southall, N. T.; Vlatchy, V.; Dill, K. A. *J. Am. Chem. Soc.* **2002**, *124*, 12302–12311.
- (39) Kalra, A.; Tugcu, N.; Cramer, S. M.; Garde, S. *J. Phys. Chem. B* **2001**, *105*, 6380–6386.
- (40) Moelbert, S.; Normand, B.; De Los Rios, P. *Biophys. Chem.* **2004**, *112*, 45–57.